

# Antibiotic-induced degradation of antitoxin enhances the transcription of acetyltransferase-type toxin-antitoxin operon

Peifei Li<sup>1</sup>, Ying-Xian Goh<sup>1</sup>, Bojana Lic<sup>1</sup>, Rui Ai<sup>1</sup>, Xinyi Meng<sup>1</sup>, Shaoyan Chen<sup>\*</sup>, Marjorie Jelic<sup>\*</sup> and Yong-Yu Yu<sup>1</sup>

<sup>1</sup>State Key Laboratory of Microbial Metabolism, Joint International Laboratory on Metabolic & Developmental Sciences, School of Life Sciences & Biotechnology, Shanghai Jiao Tong University, Shanghai 200240, China; Institute of Physics Belgrade, University of Belgrade, Belgrade 11000, Serbia; Intensive Care Unit, First Affiliated Hospital of Meical University, Oanning, Guangdong Province, 510120, China; Quantitative Biology Group, Institute of Physiology and Biochemistry, Faculty of Biology, University of Belgrade, Belgrade 11000, Serbia

\*Corresponding author. E-mail: hyou@sjtu.edu.cn

Received 14 October 2022; accepted 6 February 2023

**Background.** Bacterial toxin-antitoxin (TA) modules respond to various stressful conditions. The  $\sigma$ -related O-acetyltransferase-type toxin (AT protein encoded by the AT- locus) TA locus is involved in the antibiotic tolerance of *Klebsiella pneumoniae*.

**Objectives.** To investigate the transcriptional mechanism of the AT- operon  $\sigma$  under antibiotic stress. **Methods.** The transcriptional level of the  $\sigma$  operon of *K. pneumoniae* was measured by quantitative real-time (RT-PCR) assay. The degradation of antitoxin (acA) was examined by Western blot and fluorescent protein. The ratio of acA, acA, acT as calculated by the fluorescence intensity of acA-eGFP and mCherry-acT. Mathematical modelling predicted protein and transcript synthesis dynamics.

**Results.** A meropenem-induced increase in transcript levels of  $\sigma$  and acT resulted from the relief of transcriptional autoregulation of the  $\sigma$  operon. Meropenem induces the degradation of acA through  $\sigma$  protease resulting in a reduction in the ratio of acA, acT. The decreased ratio causes the dissociation of the acAT complex from its promoter region which eliminates the repression of  $\sigma$  transcription. In addition, our dynamic model of  $\sigma$  expression regulation quantitatively reproduced the experimentally observed reduction of the acA, acT ratio and a large increase in  $\sigma$  transcript levels under the condition of strong promoter autorepression by the acAT complex.

**Conclusions.** Meropenem promotes the degradation of antitoxin and enhancing the expression of  $\sigma$  protease. Degradation of antitoxin reduces the ratio of intracellular antitoxin:toxin leading to detachment of the TA complex from its promoter and releasing repression of TA operon transcription. These results may provide an important insight into the transcriptional mechanism of AT- TA modules under antibiotic stress.

## Introduction

After the discovery of the toxin-antitoxin (TA) modules on bacterial plasmids, these TA modules were also found on prokaryotic chromosomes.<sup>1,2</sup> Depending on the nature of the antitoxin and its interaction with the toxin, TA modules have been recently divided into eight types (types 1–8).<sup>3</sup> A typical type 4 TA module consists of a stable toxin protein and a metabolically unstable antitoxin protein forming a non-toxic TA complex.<sup>3,4</sup> Some toxins contain a  $\sigma$ -related O-acetyltransferase (AT domain) that can inhibit protein translation by acetylating aminoacyl-tRNAs such as AtaT<sup>5</sup>, AtaT8<sup>6</sup> and 4taT<sup>7</sup> from *Escherichia coli*; TacT<sup>8</sup>

TacT8 and TacT9 from *Salmonella enterica*<sup>6,8</sup> and  $\sigma$  from *Shigella flexneri*.<sup>9</sup> Their cognate antitoxin proteins possess a  $\sigma$ -helix-helix ( $\sigma$  domain). Our previous study showed that acAT is a typical AT- TA module present in the *K. pneumoniae* clinical isolate (=66873) here, acT can halt *K. pneumoniae* growth and induce antibiotic tolerance.<sup>6,36</sup>

Because TA modules are usually transcriptionally up-regulated under stressful conditions, many studies have proposed them as stress-response elements.<sup>6–8</sup> The transcription of type 4 TA operons is usually autoregulated by the toxin-antitoxin complex. In such TA modules, toxin-antitoxin complexes with different affinities for the operon region are formed due to different ratios of

antitoxin to the toxin) with antitoxin-saturated complexes show) - ing a high a<sup>nti</sup>fects their promoter.<sup>6@-86</sup> When the ratio o<sup>nti</sup> toxin to the toxin &ecomes smaller, the repression o<sup>nti</sup> TA complexes on their promoter is alle<sup>nti</sup>ated, the autoregulation o<sup>nti</sup> TA operons is relie<sup>nti</sup>ed and the translation o<sup>nti</sup> TA modules is increased.<sup>6<36@-86</sup> Ge ha<sup>nti</sup>le pre<sup>nti</sup>viously con<sup>nti</sup>drmed that anti<sup>nti</sup>biotics can increase the transcription o<sup>nti</sup> 7acT and the transcriptional le<sup>nti</sup>l o<sup>nti</sup> 7ac+T) as automatically regulated &y the , acA<sup>nti</sup>, acT ratio.<sup>6\$386</sup> (o) eler, the transcriptional mechanism and autoregulation o<sup>nti</sup> the 7ac+T operon under anti<sup>nti</sup>biotic conditions are still unclear.

The C-terminal domain or the entire antitoxin protein is o<sup>nti</sup>ten irregular and highly sensiti<sup>nti</sup>le to cellular protease. AT<sup>nti</sup>-dependent proteases ha<sup>nti</sup>le &een identi<sup>nti</sup>ed as the most important intracellular proteolytic en<sup>nti</sup>zymes, including the 2on (2a and Clp<sup>nti</sup> protease "amilies.<sup>6>388</sup> Although proteases can degrade antitoxins, e<sup>nti</sup>lidence also sho<sup>nti</sup>s that once the antitoxin "orms a sta<sup>nti</sup>ble complex) ith its cognate toxin, it) ill either not &e degraded or degraded !ery slo<sup>nti</sup>ly.<sup>8938</sup> ' ecently, a study reported that the presence o<sup>nti</sup> toxin protein IoeB and 1ps<sup>nti</sup> enhances the sta<sup>nti</sup>ility o<sup>nti</sup> antitoxin le<sup>nti</sup>1 and 1\*sA under a heat-shoc7 condition.<sup>6<</sup> (o) eler, no study has yet explored) hether , acA in the #%AT-' (( "amily can &e degraded under the anti<sup>nti</sup>biotic condition) and) hether the degradation o<sup>nti</sup> , acA is related to 7ac+T transcription.

In this study, we "ound that the increase in 7ac+T transcription induced &y the car<sup>nti</sup>apenem anti<sup>nti</sup>biotic meropenem resulted "rom the deregulation o<sup>nti</sup> 7ac+T operon autoregulation. 5egradation o<sup>nti</sup> , acA under the meropenem condition &y 2on protease reduced the ratio o<sup>nti</sup> , acA to , acT) hich caused the dissociation o<sup>nti</sup> the , acAT complex "rom its promoter region. E<sup>nti</sup>ntually, the repression o<sup>nti</sup> 7ac+T transcription &y the , acAT complex) as relie<sup>nti</sup>ed.

## Materials and Methods

### Strains and plasmids

Details o<sup>nti</sup> all the strains and plasmids used in this study are pro<sup>nti</sup>vided in Ta<sup>nti</sup>ble =6 (a<sup>nti</sup>ailable as [supplementary data](#) at J+<sup>nti</sup> Online) and all the oligonucleotides used in this study are listed in Ta<sup>nti</sup>ble =8.

### Tolerance assay

The tolerance to meropenem) as tested &y the c<sup>nti</sup>ufm2 count a<sup>nti</sup>ter exposure to meropenem. C<sup>nti</sup>ernight cultures o<sup>nti</sup> K<sup>nti</sup> pne<sup>nti</sup>&moniae strains containing di<sup>nti</sup>fferent pBA599 deri<sup>nti</sup>vaties) ere diluted in "resh 2B medium at a ratio o<sup>nti</sup> 6:6AA. Cells) ere incu<sup>nti</sup>ated at 9>JC "or 6 h and A.8K ara<sup>nti</sup>inose) as added to the cultures to induce the expression o<sup>nti</sup> the araB+D promoter. A<sup>nti</sup>ter @A min o<sup>nti</sup> incu<sup>nti</sup>ation, meropenem) as added to the cultures at \$ μgfm2. The cultures) ere incu<sup>nti</sup>ated "or another; h at the 9>JC shafter. To determine c<sup>nti</sup>ufm2 ali<sup>nti</sup>quots o<sup>nti</sup> 6AA μ2 culture) ere serially diluted and spotted on the 2B solid plates to calculate the sur<sup>nti</sup>iv<sup>nti</sup>ing cells. The sur<sup>nti</sup>iv<sup>nti</sup>al rate) as calculated &y di<sup>nti</sup>viding the c<sup>nti</sup>ufm2 in the culture a<sup>nti</sup>ter; h o<sup>nti</sup> incu<sup>nti</sup>ation) ith the meropenem &y the c<sup>nti</sup>ufm2 &e<sup>nti</sup>ore adding the meropenem.<sup>6\$3838<</sup>

### Western blot

The cells treated) ith meropenem or serine hydroxamic acid (= (L) ) ere collected and lysed &y sonication in lysis &u<sup>nti</sup>ffer (8\$ m1 Tris, \$AA m1 %aC4, \$AA μ1 phenylmethylsul<sup>nti</sup>onyl -uoride)p ( ? . A<sup>nti</sup>ter centri<sup>nti</sup>ugation, the cleared supernatant) as &oiled) ith a loading &u<sup>nti</sup>ffer "or 6A min. As "or =5--A#E and immuno<sup>nti</sup>blotting, <A Mg protein) as loaded per lane and separated &y =5--A#E using 6AK polyacrylamide gels. A<sup>nti</sup>ter

trans<sup>nti</sup>fering the separated protein to the poly<sup>nti</sup>vinylidene -uoride mem<sup>nti</sup>branes (+: 50€ 1erc7 1illipore, #ermany) the +: 50 mem<sup>nti</sup>brane) as &loc<sup>nti</sup>ted) ith 8.\$K B=A in TB=T (Tris-&u<sup>nti</sup>ffered saline) ith T) een-8A: 9A m1 Tris-&ase, A.?K %aCl) F!3 A.6K T) een-8A, p( >.\$ "or 6 h at room temperature. Then, the +: 50 mem<sup>nti</sup>brane) as) ashed three times) ith TB=T and incu<sup>nti</sup>ated) ith <x (is primary anti<sup>nti</sup>body at; JC "or a) hole night. 0ollo) ing incu<sup>nti</sup>ation, the +: 50 mem<sup>nti</sup>brane) as) ashed three times using TB=T and incu<sup>nti</sup>ated) ith the corresponding second anti<sup>nti</sup>body at room temperature "or 6 h. 0inally, the +: 50 mem<sup>nti</sup>brane) as) ashed) ith TB=T and !usual<sup>nti</sup>led &y an automatic chemiluminescence image analysis system (Tanon; <AA=0€ Tanon) =hanghai) China .

### LacZ activity assay

To construct the lacB reporter plasmid, the 7ac+T promoter se<sup>nti</sup>quence) as inserted upstream o<sup>nti</sup> the lacB gene o<sup>nti</sup> a promoterless plasmid, p2ACN3 "orming the "usion plasmid p2ACN-+7ac+T. 5i<sup>nti</sup>fferent com<sup>nti</sup>binations o<sup>nti</sup> p2ACN-+7ac+T and pBA599 plasmid) ere co-trans<sup>nti</sup>formed into ' ' 8 <7ac+T lacB- and ' ' 8 <lon 7ac+T lacB- cells. The trans<sup>nti</sup>formants) ere gro<sup>nti</sup>wn in an 2B &roth medium supplemented) ith A.8K o<sup>nti</sup> ara<sup>nti</sup>inose "or 9 h, then meropenem (\$ μgfm2 and glucose (A.8K) ) ere added. =amples "or en<sup>nti</sup>zymatic acti<sup>nti</sup>ties) ere collected at the indicated time points (A3 6\$3 9A and <A min . The β-galactosidase acti<sup>nti</sup>ty) as measured according to the standard 1 iller method using chloro<sup>nti</sup>form and =5= to per<sup>nti</sup>mea<sup>nti</sup>illite the cells.<sup>8></sup>

### Quantitative real-time (q-RT)-PCR experiments

The total %A o<sup>nti</sup> cells) as extracted according to the manu<sup>nti</sup>acturer's instructions using the %easy, it (Qiagen, #ermany . A<sup>nti</sup>ter the digestion o<sup>nti</sup> genomic 5%A using 5%ase 43 6AAA ng %A) as con<sup>nti</sup>erted to c5%A using +rime=cript<sup>nti</sup> T ' eagent, it (Ta7ara, Papan . \*+C' reaction mix (Beyo0ast<sup>nti</sup> =IB' #reen \*+C' 1ix, Category %o.: 5>8<A-6 m2) ) as purchased "rom Beyotime Biotechnology (=hanghai) China) and the reactions) ere per<sup>nti</sup>formed on an AB4 >\$AA instrument (Applied Biosystems . Each reaction) as per<sup>nti</sup>formed in triplicate simultaneously, and the "old change o<sup>nti</sup> gene expression) as calculated using the 8<sup>-ΔΔCT</sup> method.<sup>87</sup> The house<sup>nti</sup>keeping gene (glyceraldehyde-9-phosphate dehydrogenase3 K' -SC! "6"") ) as used to normal<sup>nti</sup>ize the expression le<sup>nti</sup>els o<sup>nti</sup> the di<sup>nti</sup>fferent samples.

## Results and discussion

### Meropenem induces the transcription of *kacA* and *kacT*

We Drst explored the gro<sup>nti</sup>th state o<sup>nti</sup> di<sup>nti</sup>fferent K<sup>nti</sup> pne<sup>nti</sup>&moniae strains under the meropenem condition. 0igure =6a sho<sup>nti</sup>s that, except "or the) ild-type K<sup>nti</sup> pne<sup>nti</sup>&moniae (=668?< containing the car<sup>nti</sup>apenemase gene (bla<sup>nti</sup>, +C-8) the C5<AA o<sup>nti</sup> bla<sup>nti</sup>, +C-8 gene deletion strain (=668?<- ' 8 and its deri<sup>nti</sup>ed strains) as decreased gradually a<sup>nti</sup>ter 6 h o<sup>nti</sup> treatment, meaning that cells &egan to die and lyse. Thus, we treated the strains) ith meropenem "or A3 6\$3 9A and <A min.

To see the e<sup>nti</sup>fect o<sup>nti</sup> meropenem on 7ac+T's transcription le<sup>nti</sup>l, we examined the transcription o<sup>nti</sup> 7ac+ and 7acT in K<sup>nti</sup> pne<sup>nti</sup>&moniae (=668?<- ' 8 (re<sup>nti</sup>ferred to as ' ' 8 herea<sup>nti</sup>ter) under the exposure o<sup>nti</sup> meropenem (\$ μgfm2 . At the same time, as a chemical that can stimulate a stringent response in &acteria,<sup>8@</sup> =(L (6AA μgfm2) ) as used to represent stress other than anti<sup>nti</sup>biotic stress and) as used as a comparison) ith meropenem. As sho<sup>nti</sup>n in 0igure 6, meropenem caused a signi<sup>nti</sup>ficant increase in 7acT's transcriptional le<sup>nti</sup>l, hich is consistent) ith our pre<sup>nti</sup>vious study.<sup>6\$</sup> 1eropenem also increased the transcriptional le<sup>nti</sup>l o<sup>nti</sup> 7ac+

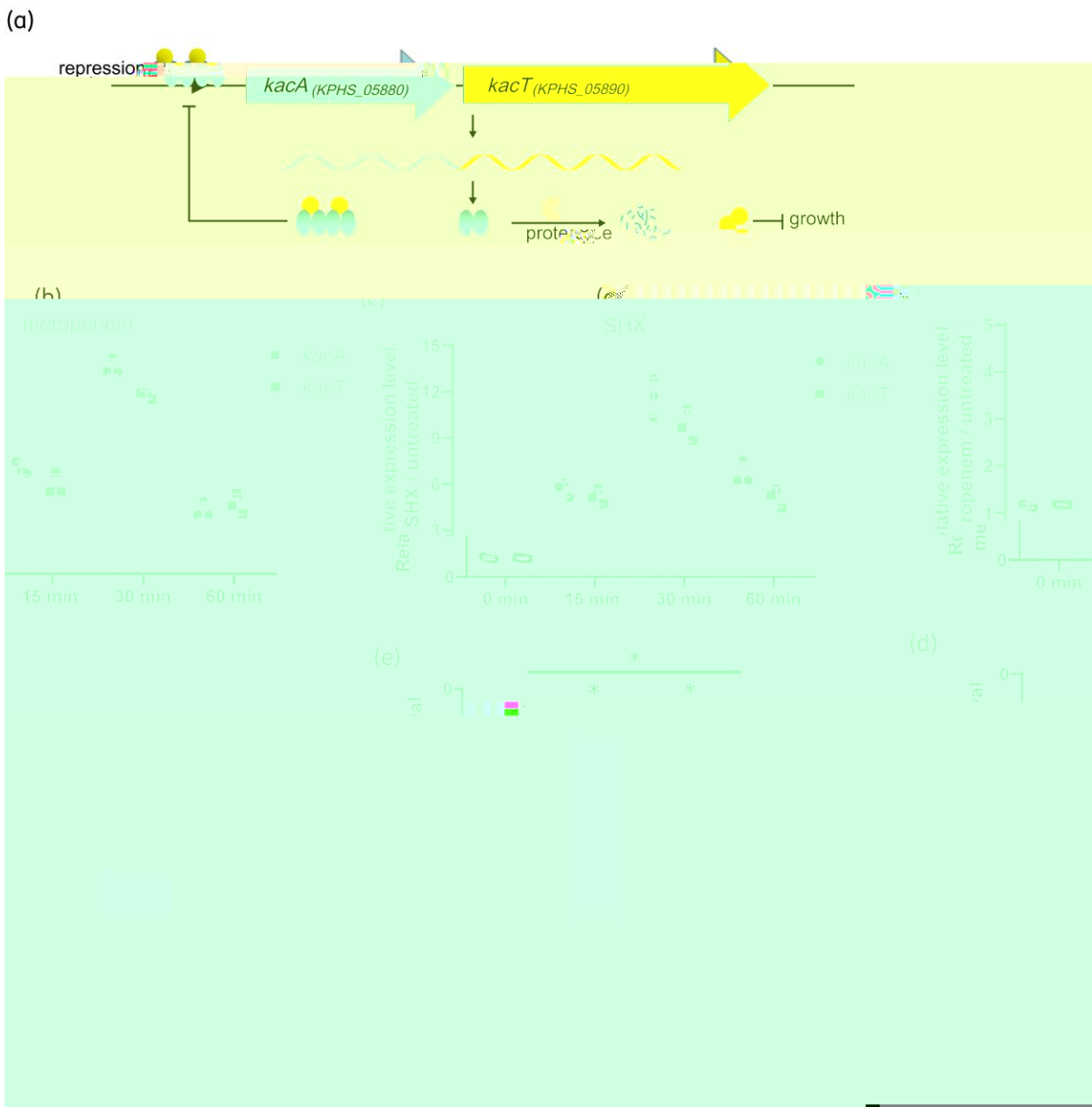


Figure 14 *kacAT* is involved in the response of *K. pneumoniae* to meropenem. (a) Schematic of acetyltransferase-type toxin-antitoxin pair *kacAT*. *kacA* and *kacT* are co-transcribed. Toxins, *kacT* molecules bind with their cognate *kacA* molecules forming a *kacAT* heterohexameric complex. The *kacAT* complex later binds and represses the *kacAT* promoter. *kacT* independently halts the growth of *K. pneumoniae* whereas, *kacA* can neutralize the toxicity of *kacT*. Proteases such as *Lon* can degrade *kacA*. Changes in *kacA* and *kacT* transcriptional levels responding to meropenem (b) or (c) are depicted as measured by qPCR. (d) The survival percentage of wild-type and *kacT* knockout strain of *kacAT* treated by meropenem (2  $\mu\text{g}/\text{mL}$  for 24 h. (e) The survival percentage of *kacAT* strains harboring empty vector pBA599, *kacT*-expressing vector (pBA599-*kacT*) or, *kacA*-expressing vector (pBA599-*kacA*) after exposure to 2  $\mu\text{g}/\text{mL}$  meropenem for 24 h. The transcriptional levels of *kacA* and *kacT* genes were normalized using the house-keeping gene *gapA*. The survival percentage was calculated by dividing the CFU of the meropenem-treated culture by the CFU of the culture before adding meropenem. (L) as used to compare with meropenem. The bar represents the mean of three independent experiments and the error bar indicates the  $\pm 5$  (\*  $p$  value  $< 0.05$ ). This figure appears in colour in the online version of *J+* and in black and white in the print version of *J+*.

(Figure 6b. On the other hand, the transcriptional levels of *kacA* and *kacT* were also significantly enhanced by (Figure 6c. These results indicated that, similar to other families of TA modules, the *kacAT*-type TA module, *kacAT*, also responded to different stress conditions.

**Overexpression of *kacAT* operon enhances the tolerance of *K. pneumoniae* to meropenem**

The expression of the toxin gene *kacT* significantly inhibited the growth of *K. pneumoniae* whereas the expression of *kacA* or

Meropenem affects 7ac+T transcription

empty pBA599 plasmid did not (Figure 6b and c). Additionally, we previously found that, acT overexpression induced meropenem tolerance in *K. pneumoniae*.<sup>65</sup> However, the effect of the 7ac+T operon on meropenem tolerance remains to be elucidated. We examined whether the 7ac+T operon affects meropenem tolerance in '18. As Figure 6d shows, the survival of '18 under meropenem exposure was not affected, disregarding the presence of the 7ac+T operon. It is worth noting that, except for acT overexpression, acAT also induced meropenem tolerance in '18.

(Figure 9a and b). Using the wild-type  $\Delta lon$  and  $\Delta lon$  strains, we further examined the effect of Lon on  $7ac+$  transcription after meropenem exposure. Our results showed that the transcription levels of  $7ac+$  and  $7acT$  in the  $\Delta lon$  strain were remarkably lower than in the wild-type  $\Delta lon$  strain after meropenem or  $\beta$ -L exposure (Figure 9c and d). These results suggest that Lon is transcribed at a higher rate under meropenem exposure, possibly translating more Lon protease that could affect  $7ac+$  and  $7acT$  transcription.

### **Meropenem leads to KacA degradation through Lon protease**

The in vivo degradation rate of  $KacA$  was examined. Ge Drst used

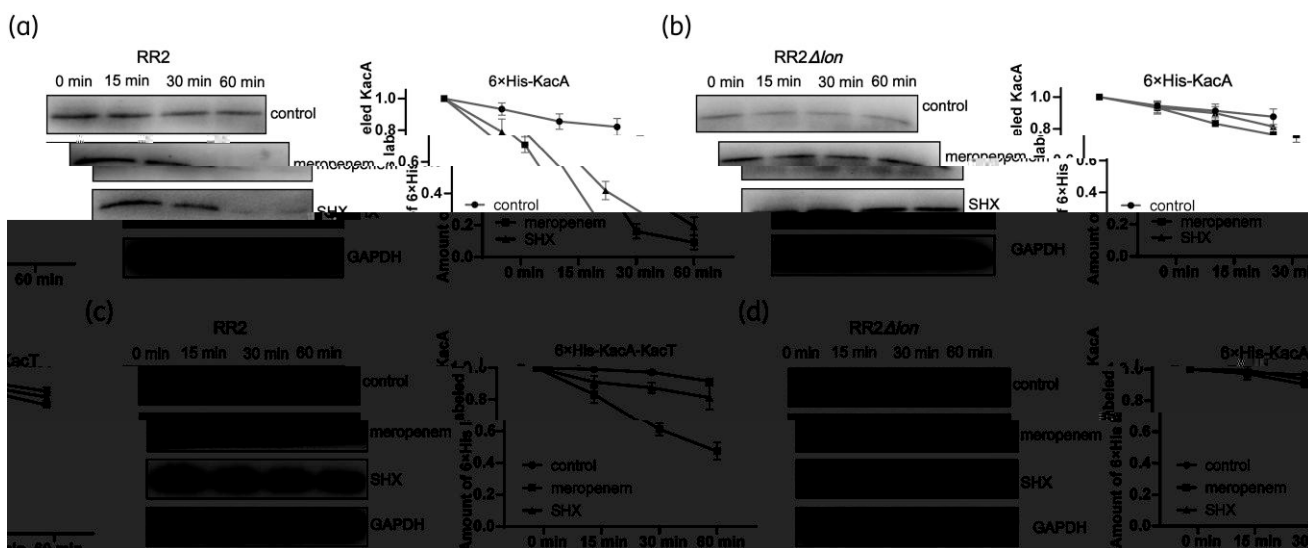


Figure 4 1 eropenem induces KacA degradation through Lon protease. Wild-type RR2 and Lon-deletion (RR2Δlon) strains harboring the pBA599 vector that expresses (a) only KacA and (c) KacA and KacT, with A.8K (10% D-glucose) as added to inhibit KacA expression together with meropenem. Samples were collected at the indicated time points (0, 15, 30, 60 min) and (c and d show) that KacA is degraded by Lon protease after meropenem exposure. (b and d show) that KacA could not stabilize under meropenem exposure. SHX (SH) was used to compare with meropenem. Data are presented as mean ± SD (error bars) (n = 9). #A+5 (3-hydroxyaldehyde-9-phosphate dehydrogenase).

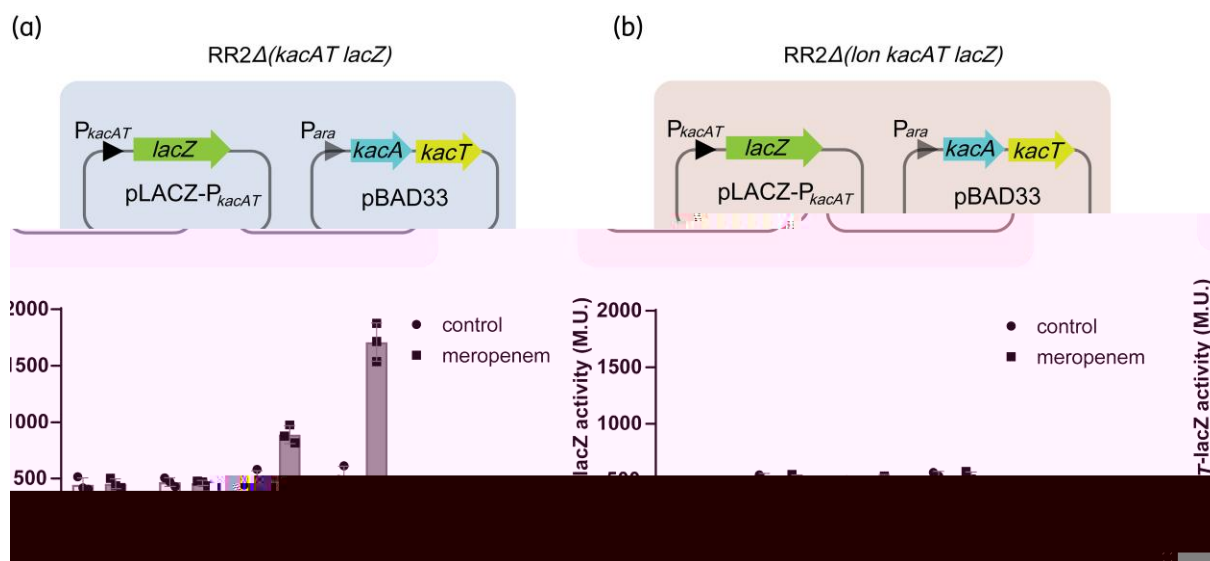


Figure 5 1 eropenem promotes the dissociation of the KacA-KacT complex from its promoter. 7ac+T promoter (+7ac+T and the downstream lacB) were cloned on the p2ACN-7ac+T plasmid whereas 7ac+ and 7acT were on the pBA599 plasmid. p2ACN-7ac+T and pBA599 in combination expressing KacA and KacT were co-transformed into RR2Δ7ac+T lacB (a) and RR2Δlon 7ac+T lacB (b) cells. 1 eropenem and A.8K glucose were added after 9 h of induction of KacA and KacT by arabinose (A.8K). Samples were collected at the indicated timepoints (0, 15, 30, 60 min). 1 R3 miller unit. This figure appears in colour in the online version of JAC and in black and white in the print version of JAC.

meropenem or (L3 the fluorescence intensity of KacA-e#0+) as significantly decreased in the wild-type RR2 compared with RR2Δlon cells (Figure 5b and c). Despite the presence of KacT the fluorescence intensity of KacA-e#0+ in wild-type RR2) as still significantly reduced after meropenem treatment compared

with the RR2Δlon strain (Figure 5d and e) which is consistent with the results of Western blot. Besides we also found that meropenem caused reduced fluorescence intensity of KacA-e#0+ in wild-type RR2 compared with RR2Δlon cells) which implies that meropenem can also induce the degradation of KacA (Figure 5f).



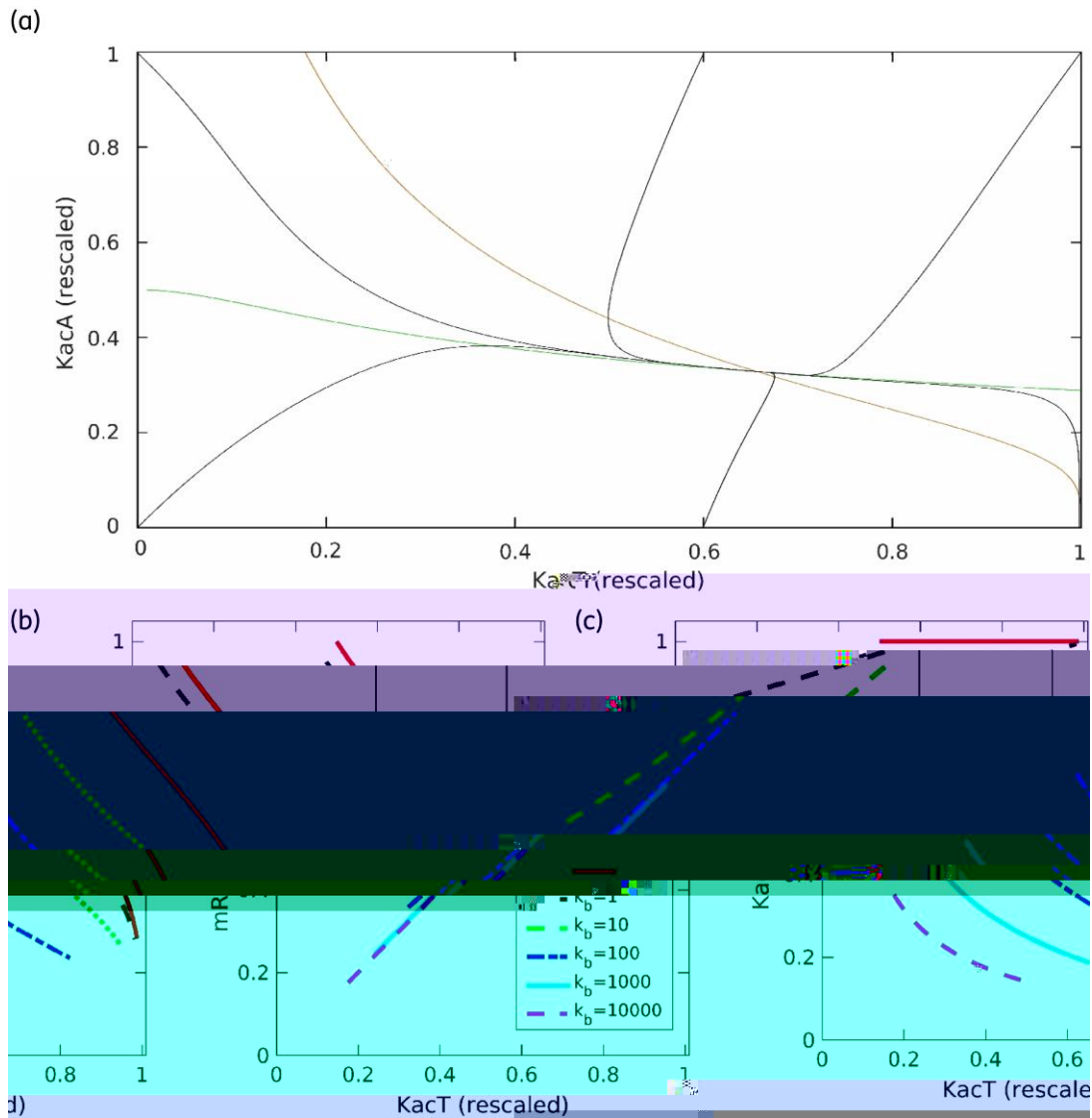


Figure 6: Phase plane analysis of the system dynamics for the rescaled parameter values  $\tilde{K}_T = 63$ ,  $\tilde{K}_B = 6AA3$ ,  $\Delta = 9$  (see Materials and Methods). The orange and green curves correspond to  $KacA$  and  $KacT$  nullclines, respectively, with their intersection determining the system's steady state. Solid black curves present trajectories for different system initial conditions (a). Equilibrium values of  $KacA$  versus  $KacT$  (b) and  $KacA$  versus  $KacT$  (c). Different curves correspond to different  $K_B$  values indicated in the legend. Points on each curve correspond to changing  $\Delta$  from A (left edge) to C (right edge) and the values on the axes are rescaled. This figure appears in colour in the online version of J+\$. and in black and white in the print version of J+\$. .

Additionally, we studied whether meropenem could induce  $KacT$ 's degradation. Under meropenem treatment, the non-toxic,  $KacT^{16:50}$  in  $\Delta$  or  $\Delta$  lon did not degrade much (Figure 2a and b, 2i7e) since the fluorescence intensity of mCherry-,  $KacT^{16:50}$  in wild-type  $\Delta$  did not change after meropenem treatment (Figure 2c and d).

### Meropenem promotes dissociation of the KacAT complex from its promoter

Because meropenem can promote the degradation of  $KacA$  and not  $KacT$ , meropenem likely alters the intracellular ratio of  $KacA$  to  $KacT$ . To our knowledge, the change in antitoxin to toxin

ratio has not been successfully investigated in vivo although some approaches have been tried such as the pulse-chase assay.<sup>6c</sup> We initially used Western blotting to explore changes in the  $KacA$  to  $KacT$  ratio but also failed (data not shown). (ence) We used  $KacA$  and  $KacT$  with e#0+ and mCherry, respectively. The fluorescence intensity of  $KacA$ -e#0+ and mCherry-,  $KacT$  under meropenem stress) as measured by a microplate reader. Our results showed that the ratio of remaining  $KacA$ -e#0+ to mCherry-,  $KacT$  as significantly reduced in the wild-type  $\Delta$  under the meropenem condition (Figure 2a, 1e) while the ratio of  $KacA$  to  $KacT$  in the lon deletion strain remained unchanged (Figure 2c & d).

Due to the reduced ratio of  $\lambda$ acA/::, acT/ caused by meropenem, we suggest that meropenem can promote the dissociation of the  $\lambda$ acAT complex from its promoter region. We performed a 2acN activity experiment in the  $\lambda$ ac+T promoter ( $+\lambda_{ac+T}$ ). Our results showed that with the prolongation of meropenem treatment time, 2acN activity in  $\lambda$ ac+T lacB<sup>-</sup> harboring  $\lambda$ acA and  $\lambda$ acT increased, whereas the  $\lambda$ ac+T lacB<sup>-</sup> did not (Figure 5). Additionally, in  $\lambda$ ac+T lacB<sup>-</sup> and  $\lambda$ ac+T lacB<sup>-</sup> containing the empty pBA599 plasmid, 2acN activity was also unchanged under the meropenem conditions (Figure 6). A plausible explanation is that under meropenem conditions, the  $\lambda$ acAT complex dissociates from its promoter  $+\lambda_{ac+T}$  leading to the transcription of 2acN.

### A quantitative model of $\lambda$ acAT expression dynamics explains experimental observations

Based on the experimental results presented above, we developed a quantitative model that can predict protein and transcript synthesis dynamics (see supplemental methods). We aimed to achieve the following through the model: (1) Check if and under what conditions (parameter range) the model can explain the experimentally observed system response to anti-infective stress, in particular, the significant increase in  $\lambda$ ac+T transcript amounts and the decrease in  $\lambda$ acA/::, acT/ ratio. (2) Predict the dynamics of  $\lambda$ acT under anti-infective stress, i.e. upon an increase in  $\lambda$ acA degradation. In particular, we aimed to understand the somewhat perplexing observation that  $\lambda$ acAT overexpression induces anti-infective stress tolerance, whereas  $\lambda$ ac+T deletion does not affect this tolerance. (3) Infer general properties of  $\lambda$ ac+T expression

dynamics, such as the steady state number and stability, and how the steady states change with changing parameter values (which is also related to the topic of previous points).

We start with (9) and (10) with Figure 7a presenting the phase space analysis of the system dynamics. The system has one steady state corresponding to the intersection of the two nullclines (the orange and the green curves). Linear stability analysis leads to two negative real eigenvalues for this steady state, corresponding to a stable node. Figure 7a shows that trajectories with different initial conditions converge to this stable node. As the system parameters are changed, the phase space topology does not change, but the position of the steady state changes its location in the phase space (not shown in Figure 7a).

We next analyse how the steady state changes as  $\Delta$  (scaled degradation rate of  $\lambda$ acA and  $\tilde{K}_B$  (scaled binding affinity of  $\lambda$ acAT complex to the promoter) are changed.  $\Delta$  is similar to the experimental analysis, found that this parameter, the anti-infective stress influences the system dynamics, where  $\Delta$  is changed from A (the absence of anti-infective stress) to the relatively high value of  $\Delta = 1$ . It is also clear that  $\tilde{K}_B$  is a crucial parameter controlling system behaviour given the reported derepression of the promoter upon anti-infective stress.  $\tilde{K}_B = A$  corresponds to a constitutive (unregulated promoter) condition in investigation of the system's behaviour during overexpression experiments. Similarly, high values of  $\Delta$  and  $\tilde{K}_B$  correspond to the high values of  $\lambda$ acA/:: and  $\lambda$ acT/ ratio.



right edge to  $\Delta \sim <3$  and different curves correspond to different  $K_B$  values (see the legend in Figure 4). We see that irrespective of the  $K_B$  the ratio  $\Delta$ ,  $\text{acA}/\text{acT}$  decreases as  $\Delta$  increases consistently with experimental observations. Therefore, we obtain a robust (independent of parameter values) prediction that antibiotic stress leads to decreased  $\text{acA}$  and increased  $\text{acT}$ . This prediction is non-trivial because the decrease of the  $\Delta$ ,  $\text{acA}/\text{acT}$  ratio can also be realized through other scenarios, e.g. if  $\text{acT}$  remains constant or even decreases accompanied by a "aster decline" of  $\text{acA}$ .

Figure 4 shows  $\text{acA}$  and  $\text{acT}$  steady-state values. Five different lines correspond to different  $K_B$  values and points on each line correspond to increasing (from left to right along the lines)  $\Delta$  values. The horizontal (topmost) line corresponds to the constitutive promoter ( $K_B = A$ ) i.e. to the conditions of the overexpression experiment. The figure shows that smaller  $K_B$  values do not lead to a significant increase in the transcript amounts, contrary to what was experimentally observed. Consequently, the strong binding of the complex to the promoter (high  $K_B$  values is consistent) with the experimental results. Interestingly, for high  $K_B$  values (see the bottommost line corresponding to  $K_B = 6A$ ) the highest value of  $\Delta$ ,  $\text{acT}$  (the right edge of the line) obtained "or the highest value of  $\Delta$  is still smaller than the lowest value (the left line edge corresponding to  $\Delta = A$  in the constitutive case. This prediction might explain the naturally surprising result that the overexpression experiment led to antibiotic stress tolerance, which is not the case for the native (autoregulated) system. That is due to the strong binding of the repression complex to promoter  $\text{acA}$  leading to a significant increase in  $\text{acA}$  degradation rate might not be enough to achieve large enough  $\text{acT}$  levels necessary to observe antibiotic tolerance.

### Transcriptional mechanism of the *kacAT* operon under meropenem stress

Based on the above, we propose a putative model that explains the transcriptional mechanism of the  $\text{acA}$  operon under the meropenem condition (Figure 5). In normal circumstances, the relatively low  $\text{acT}$  translation efficiency of  $\text{acT}$  ensures the amount of  $\text{acA}$  molecules is more than that of  $\text{acT}$ .  $\text{acA}$  molecules counteract all  $\text{acT}$  molecules to form the  $\text{acAT}$  complex without releasing the toxicity of  $\text{acT}$ . The  $\text{acAT}$  complex can bind to its promoter region and block the transcription of  $\text{acA}$ . Once the limiting conditions are changed, such as in meropenem stress, the transcriptional level of the  $\text{acA}$  gene is increased, resulting in the degradation of unstable  $\text{acA}$ . Due to the degradation of  $\text{acA}$ , the ratio of  $\Delta$ ,  $\text{acA}/\text{acT}$  becomes  $<1$  and the  $\text{acAT}$  complex subsequently dissociates from the promoter region of the  $\text{acA}$  operon, thereby relieving repression of  $\text{acA}$  transcription.

### Funding

This work was supported by the National Natural Science Foundation of China (grant no. 81873001) and the Science and Technology Commission of Shanghai Municipality (grant no. 17010702000) and the Medical Engineering Cross Research Fund of Shanghai Piao Tong University (18010702000) and the National Natural Science Foundation of China (grant no. 81873001) and the Medical Excellence Award Funded by the

Chinese Academy of Sciences (grant no. 2018YFA0900100) and the National Natural Science Foundation of China (grant no. 81873001) and the Medical Excellence Award Funded by the

### Transparency declarations

All authors: none to declare.

### Supplementary data

Figures 6 to 8 and supplemental methods are available as supplementary data at JMI Online.

### References

1. Herdes, J, Smussen, B, Olin, R. R. Plasmid maintenance function: postsegregational killing of plasmid-free cells. *Proc Natl Acad Sci U S A* 2001; 98: 966-970. <https://doi.org/10.1073/pnas.98.4.966>
2. Lie, J, Geis, J, Hen, I, et al. TA5B8A: an updated database of bacterial type 44 toxin-antitoxin loci. *Oncleic + ci (s 3es 8A67E \*6: 5); @B5\$9*. <https://doi.org/10.1093/fnarfg7x6A99>
3. Hao, J, Arrison, E, Bi, S, et al. TA5B8A: a eukaryotic resource for type 8 toxin-antitoxin loci in bacteria and archaea. *Oncleic + ci (s 3es 8A66E &8: 5<A<B566*. <https://doi.org/10.1093/fnarfg7x6A99>
4. Purnas, S, Orain, J, Noormaghtigh, O, et al. Biology and evolution of bacterial toxin-antitoxin systems. *Oat 3ev Microbiol* 8A88E 19: 99-108. <https://doi.org/10.1093/fnarfg7x6A99>
5. Arms, A, Brodersen, S, Mitarai, N, et al. Toxins, targets, and triggers: an overview of toxin-antitoxin biology. *Mol Cell* 8A67E 09: 20-30. <https://doi.org/10.1016/j.molcel.2012.06.009>
6. Page, J, et al. G. Toxin-antitoxin systems in bacterial growth arrest and persistence. *Oat Chem Biol* 8A66E 11: 8A7B6; . <https://doi.org/10.1016/j.ccr.2012.06.009>
7. Purnas, S, Chatterjee, S, Onijn, A, et al. Ataxin translation initiation and acetylation of the initiator tRNA<sup>Met</sup>. *Oat Chem Biol* 8A66E 11: 8A7B6; . <https://doi.org/10.1016/j.ccr.2012.06.009>
8. Chinn, T, et al. The mechanism of translation inhibition by type 44 toxin-antitoxin systems. *Oncleic + ci (s 3es 8A8A E \*1: 2<6>B8\$*. [https://doi.org/10.1093/fnarfg7aa5\\$6](https://doi.org/10.1093/fnarfg7aa5$6)
9. Gilcox, B, Csterman, J, Erya, A, et al. *Escherichia coli* 4taT is a type 44 toxin that inhibits translation by acetylating isoleucyl-tRNA<sup>Ile</sup>. *Oncleic + ci (s 3es 8A67E \*6: >?>9B?\$. [https://doi.org/10.1093/fnarfg7y\\$<A](https://doi.org/10.1093/fnarfg7y$<A)*
10. Che, L, et al. Salmonella toxin promotes persistence through acetylation of tRNA. *Mol Cell* 8A66E 11: 8A7B6; . <https://doi.org/10.1016/j.molcel.2012.06.009>
11. Coyle, P, et al. The role of acetyltransferase toxins in the persistence of Salmonella during macrophage infection. *Oat Somm n 8A67E 8: 6@@9*. <https://doi.org/10.1093/fnarfg7x6A99>
12. Erya, A, et al. Auxiliary interactions support the evolution of specific toxin-antitoxin pairing. *Oat Chem Biol* 8A86E 10: 68-74. <https://doi.org/10.1016/j.ccr.2012.06.009>
13. Cicerone, T, Tang, C. Evolution of toxin-antitoxin systems in the evolution of *Shigella sonnei* as a host-adapted pathogen. *Oat Microbiol* 8A66E 11: 6<8A; . <https://doi.org/10.1093/fnarfg7x6A99>
14. Zhai, J, et al. Complete genome sequence of *Klebsiella pneumoniae* subsp. *pneumoniae* (6687) a multidrug-resistant strain isolated from human sputum. *J Bacteriol* 8A68E 18\*: 67; 6B8. <https://doi.org/10.1128/JB.01111-08>

## 1 eropenem a""ects 7ac+T transcription

- 15 Oian (3 Iao O3 Tai C et al8 4dentiDcation and characteriHation o" acetyltrans"erases-type toxin-antitoxin locus in Klebsiella pne&moniae. Mol Microbiol 8A6?E 191: 99<B; @. https://doi.org/6A.6666fmmi.69@9;
- 16 2e' oux 13 Cul!iner +(3 2iu IP et al8 =tress can induce transcription o" toxin-antitoxin systems ) ithout acti!ating toxin. Mol Sell 8A8AE 08: 87AB@8. https://doi.org/6A.6A6<fj.molcel.8A8A.A\$.A8?
- 10 1 uthuramalingam 13 Ghite PC3 Bourne C'. Toxin-antitoxin modules are plia&le s) itches acti!ated &y multiple protease path) ays. To/ins <Basel= 8A6<E 1: 86; . https://doi.org/6A.99@Aftoxins?A>A86;
- 11 ' onneau =3 (elaine =. Clari"ying the lin7 &et) een toxin-antitoxin mod- ules and &acterial persistence. J Mol Biol 8A6@E \* &1: 9; <8B>6. https://doi. org/6A.6A6<fj.jm&.8A6@.A9.A6@
- 18 C!ergaard 13 Borch P3 Porgensen 1 # et al8 1 essenger ' %A inter"erases ' eIE controls relB9 transcription &y conditional cooperati! ity. Mol Microbiol 8AA?E 68: ?; 6B\$>. https://doi.org/6A.6666fj.69<\$-8@\$.8AA?.A<969.x
- ! 9 #arcia-+ino A3 Balasu&ramanian =3 Gyns 2 et al8 Allostery and intrinsic disorder mediate transcription regulation &y conditional cooperati! ity. Sell 8A6AE 1\*! : 6A6B66. https://doi.org/6A.6A6<fj.cell.8A6A.A\$.A9@
- ! 1 Oian (3 Iu (3 2i + et al8 Toxin-antitoxin operon 7ac+T o" Klebsiella pne& moniae is regulated &y conditional cooperati! ity !ia a G-shaped , acA-, acT complex. O&cleic +ci(s 3es 8A6@E \*0: ><@AB>A8. https://doi. org/6A.6A@9fnarf7H\$<9
- !! Bordes +3 #ene! aux +. Control o" toxin-antitoxin systems &y proteases in Mycobacteri&m t&berc&losis. \*ront Mol Biosci 8A86E 1: <@69@@. https:// doi.org/6A.99?@F"mol&.8A86.<@69@@
- ! & 5u&iel A3 GegrHyn , 3 , upins7i A+ et al8 ClpA+ protease is a uni!ersal "actor that acti!ates the parD9 toxin-antitoxin system "rom a broad host range ' , 8 plasmid. Sci 3ep 8A6?E 1: 6\$8?>. https://doi.org/6A. 6A9?Fs; 6\$@?-A6?-99>8<-y
- ! \* 2unge A3 #upta ' 3 Choudhary E et al8 The un"oldase ClpC6 o" Mycobacteri&m t&berc&losis regulates the expression o" a distinct su&set o" proteins ha!ing intrinsically disordered termini. J Biol \$hem 8A8AE ! 85: @; \$B>9. https://doi.org/6A.6A>; Fj&c.' A68A.A69; \$<
- ! 5 1 aisonneau! e E3 =ha7espeare 2P3 Porgensen 1 # et al8 Bacterial persist- ence &y ' %A endonucleases. ' roc Oatl +ca( Sci S + 8A66E 191: 698A<B66. https://doi.org/6A.6A>9fnpnas.66AA6?<6A?
- ! 6 +u l3 Nhao N3 2i l et al8 Enhanced e"-ux acti! ity "acilitates drug toler- ance in dormant &acterial cells. Mol Sell 8A6<E 6! : 8?; B@; . https://doi.org/ 6A.6A6<fj.molcel.8A6<.A9.A9\$
- ! 0 #ri"Dth , 23 Gol" ' E. 1 easuring &eta-galactosidase acti! ity in &acteria: cell gro) th3 permea&iliHation3 and enHyme assays in @<-) ell arrays. Biochem Bioph 3es \$o 8AA8E ! 89: 9@>B; A8. https://doi.org/6A.6AA<F &&rc.8AA6.<6\$8
- ! 1 2i! a7 , P3 =chmittgen T5. Analysis o" relative gene expression data using real-time \*uantitati!e +C' and the 8- $\Delta\Delta\text{CT}$  method. Metho(s 8AA6E ! 5: ; A8B?. https://doi.org/6A.6AA<fmeth.8AA6.68<8
- ! 8 (addadin OT3 , urth (3 ( arcum =G. =erine hydroxamate and the tran- scriptome o" high cell density recom&inant 9scherichia coli 1 #6<\$\$. +ppl Biochem Biotechnol 8AA@E 150: 68; B9@. https://doi.org/6A.6AA>Fs68A6A- AA?-?8; 6-A
- &9 Nhou L3 Ec7art 1 ' 3 =hapiro 2. A &acterial toxin pertur&s intracellular amino no(amino nothiJi/T 1277 (& (pN22o - 1.24T 128 15.999826.5 (n026 ) 3m3 -



95 **Supplemental methods**

94

97

06 ! T

09 °C

00

01 T T54

02 T T54

\*

03

\*

04

TVG

05 C FR ( ,

TV4 G

C FR (

C FR ( ,

04

TVG

TV4 G

07

K.

16 *pneumoniae* HS11286

19

FTV

10

TVG

TV4 G

11 ) TV4

) TV4 G

V TVG

12

HS11286-RR2 or HS11286-RR2 TV4 G

13

14

15

14

17

26  
29  
20  
21  
22  
23  
24  
25  
24  
27  
36  
39  
30  
31  
32  
33  
34  
35  
34  
37  
46  
49  
40

*K. pneumoniae* HS11286-

HS11286-

TV4 G

TV4 G

TV4 G

TV4

**Figure 2A**

TV5

TV5

TV4

TV4

TVG

TV4 : 9C

6

TVG

8! V

\*

41

42

43

44

TV4 TVG

45

44

°C

47

56

59

50

51

52

$m$

$\varphi$

53

$\lambda_m$

54

$$\frac{dm}{dt} = \varphi - \lambda_m m.$$

(1.1)

55

54  $dm / dt = 0$

57

$$m = \frac{\varphi}{\lambda_m}.$$

(1.2)

46

49

$\varphi_0$

40

$$m = \frac{\varphi_0}{\lambda_m}.$$

(1.3)

41

' 4 G 4

42  
43  
44  
45  
44  
47  
76  
79  
70  
71  
72  
73  
74  
75  
74  
77  
966  
969  
960  
961

G

$$\varphi = \frac{\varphi_0}{1 + \frac{[4A2T]}{K_D}}, \quad (1.4)$$

$\varphi_0$   $[4A2T]$

$K_D$

$$\frac{dA}{dt} = K_A m - (\lambda_C + \Delta\lambda)A - 4\lambda_C [4A2T], \quad (1.5)$$

$$\frac{dT}{dt} = K_T m - \lambda_C T - 2\lambda_C [4A2T], \quad (1.6)$$

$K_A$   $K_T$   $\lambda_C$

$\Delta\lambda$

A

A G

$4A2T$



962  $4A + 2T \xrightleftharpoons[K_-]{K_+} [4A2T] \xrightarrow{\lambda_c} 0,$  (1.7)

963  $d[4A2T]/dt = 0$

964  $K_+ A^4 T^2 - K_- [4A2T] - \lambda_c [4A2T] = 0.$  (1.8)

965

964

967  $[4A2T] = \frac{K_+}{K_-} A^4 T^2 = \frac{A^4 T^2}{K^5},$  (1.9)

996  $K^5 \equiv K_- / K_+ \quad K$

999

990  $dA/dt$

991  $dT/dt \quad A \quad T$

992  $K_A = 2K_T \quad A \quad T \quad 4A2T$

993

994  $4 \square \quad G \square$

995

994  $A^* = \frac{2\lambda_c}{\lambda_c + \Delta\lambda} T^*.$  (1.10)

997  $A^* \quad T^*$

906

909

900

901

902

903

904

$$\tilde{m} = m / K \quad \tilde{A} = A / K \quad \tilde{T} = T / K$$

905

TV4 G

904

$$\tau = \lambda_c t$$

907

$$\lambda_c \quad \tilde{K}_T = K_T / \lambda_c \quad \Delta \tilde{\lambda} = \Delta \lambda / \lambda_c \quad \tilde{K}_B = K / K_D$$

916

$$4A2T \quad A4 \quad \tilde{\varphi} = \varphi_0 / (\lambda_m K)$$

919

910

911

$$\frac{d\tilde{A}}{d\tau} = 2\tilde{K}_T \tilde{m} - (1 + \Delta \tilde{\lambda}) \tilde{A} - 4\tilde{A}^4 \tilde{T}^2 \quad (1.11)$$

912

$$\frac{d\tilde{T}}{d\tau} = \tilde{K}_T \tilde{m} - \tilde{T} - 2A^4 T^2. \quad (1.12)$$

913

914

915

914

917

926

929

920

TV4 G

921

$$\tilde{K}_B \quad 4A2T \quad \Delta \tilde{\lambda}$$

922

923  $\tilde{T}^*$

924

925 
$$0 = K_T \frac{\varphi}{1 + K_B \frac{2}{1 - \lambda} T^{*6}} T^* 2 \left( \frac{2}{1 - \lambda} \right)^4 T^{*6}. \quad (1.13)$$

924

927  $\tilde{T}^* \quad \tilde{A}^* \quad \tilde{m}^*$

936 
$$\tilde{A}^* = \frac{2}{1 + \Delta\tilde{\lambda}} \tilde{T}^*, \quad (1.14)$$

939

930 
$$\tilde{m}^* = \frac{\tilde{\varphi}}{1 + \tilde{K}_B \left( \frac{2}{1 + \Delta\tilde{\lambda}} \right)^4 \tilde{T}^{*6}}, \quad (1.15)$$

931 
$$\tilde{K}_B = 0$$

932

933  $\tilde{A}^* \quad \tilde{T}^* \quad \tilde{m}^* \quad \tilde{K}_B \quad \Delta\tilde{\lambda}$

934 **Statistical analysis**

935

934

937 C

946

949

940

941 **Table S1.**

Strain/plasmid	Description	Source or Reference
<b>Strain</b>		
<i>K. pneumoniae</i> :		
	T C FR ( C FR T	4
		This study
TV4 G	TV4 G	This study
TV4 G TVM	TV4 G TVM	This study
TV4 G TVM	TV4 G T TVM	This study
8! V -		
8! V	G T V F5	Novagen
<b>Plasmid</b>		
pBAD33	p15A ori; araC; Para promoter, Cml <sup>R</sup>	5
pBAD33+ <i>kacT</i>	pBAD33 bearing <i>kacT</i> and its SD sequence as an <i>SacI-HindIII</i> insert	This study
pBAD33+ <i>kacAT</i>	pBAD33 bearing <i>kacAT</i> and its SD sequence as an <i>SacI-HindIII</i> insert	This study
pBAD33+6xHis- <i>kacA</i>	pBAD33 bearing 6xHis labeled <i>kacA</i> and its SD sequence as an <i>SacI-HindIII</i> insert	This study
pBAD33+6xHis- <i>kacA-kacT</i>	pBAD33 bearing 6xHis labeled <i>kacA</i> with <i>kacT</i> and its SD sequence as an <i>SacI-HindIII</i> insert	This study
pBAD33+Myc- <i>kacT</i> <sup>Y145F</sup>	pBAD33 bearing Myc labeled <i>kacT</i> <sup>Y145F</sup> and its SD sequence as an <i>SacI-HindIII</i> insert	This study
pBAD33+ <i>kacT-mCherry</i>	pBAD33 bearing <i>kacT-mCherry</i> as an <i>SacI-HindIII</i> insert	This study
pBAD33+ <i>mCherry-kacT</i>	pBAD33 bearing <i>mCherry-kacT</i> as an <i>SacI-HindIII</i> insert	This study
pBAD33+ <i>kacT+eGFP-kacA</i>	pBAD33 bearing <i>kacT</i> with <i>eGFP-kacA</i> as an <i>SacI-HindIII</i> insert	This study
pBAD33+ <i>kacT+kacA-eGFP</i>	pBAD33 bearing <i>kacT</i> with <i>kacA-eGFP</i> as an <i>SacI-HindIII</i> insert	This study
pBAD33+ <i>mCherry-kacT+kacA</i>	pBAD33 bearing <i>mCherry-kacT</i> with <i>kacA</i> as an <i>SacI-HindIII</i> insert	This study
pBAD33+ <i>mCherry-kacT+eGFP-kacA</i>	pBAD33 bearing <i>mCherry-kacT</i> with <i>eGFP-kacA</i> as an <i>SacI-HindIII</i> insert	This study
pBAD33+ <i>mCherry-kacT+kacA-eGFP</i>	pBAD33 bearing <i>mCherry-kacT</i> with <i>kacA-eGFP</i> as an <i>SacI-HindIII</i> insert	This study
pBAD33+ <i>kacA-eGFP</i>	pBAD33 bearing <i>kacA-eGFP</i> as an <i>SacI-HindIII</i> insert	This study
pBAD33+ <i>kacA-eGFP-kacT</i>	pBAD33 bearing <i>kacA-eGFP</i> with <i>kacT</i> as an <i>SacI-HindIII</i> insert	This study
pCD (pCDFDuet)	T7 promoter, KanaR	Novagen
pCD+ <i>mCherry-kacT+kacA-eGFP</i>	pCD bearing <i>mCherry-kacT</i> with <i>kacA-eGFP</i> as an <i>SacI-HindIII</i> insert	This study
pLacZ-P <sub><i>kacAT</i></sub>	pLACZ derivative with promoter of <i>kacAT</i> operon inserted upstream of <i>lacZ</i>	This study

---

**Name**

---

KacTF

KacTR

KacATF

Y145F

Y145R

RTkacTF

RTkacTR

RTkacAF

RTkacAR

RTgapAF

RTgapAR

KacAEF

KacAER

KacTEF

KacTER

mkacTF

mkacTR

KacTmF

KacTmR

ekacAF

ekacAR

NkacAEF

NkacAER

CkacAEF

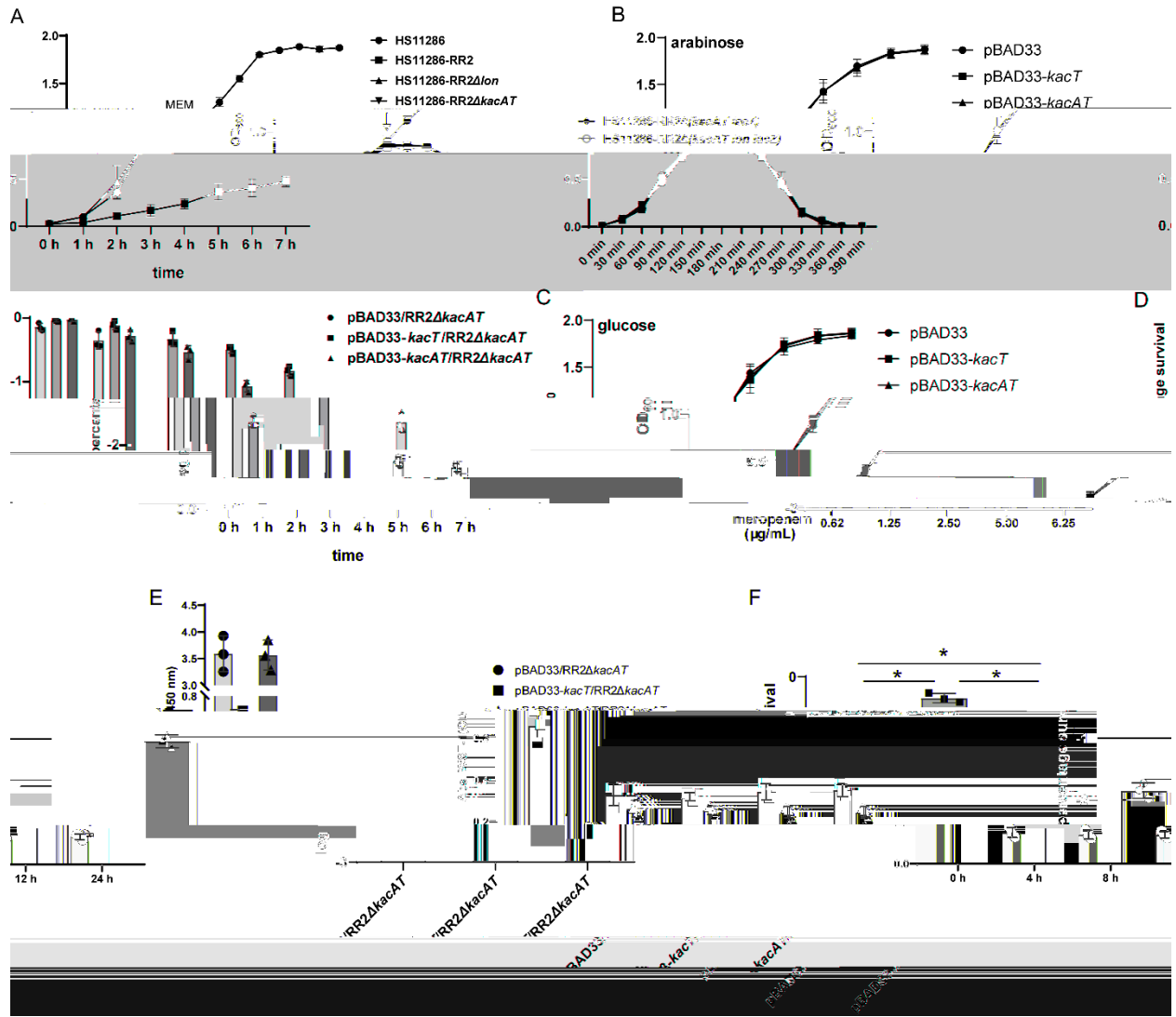
CkacAER

NkacTMF

NkacTMR

CkacTMF

CkacTMR



945

944 **Figure S1.**

947 **A**

956

959

950 **B-C**

951

952 **TV4G**

953 TVG

TV4G

954

E

955

!

T

TV4G

954

957

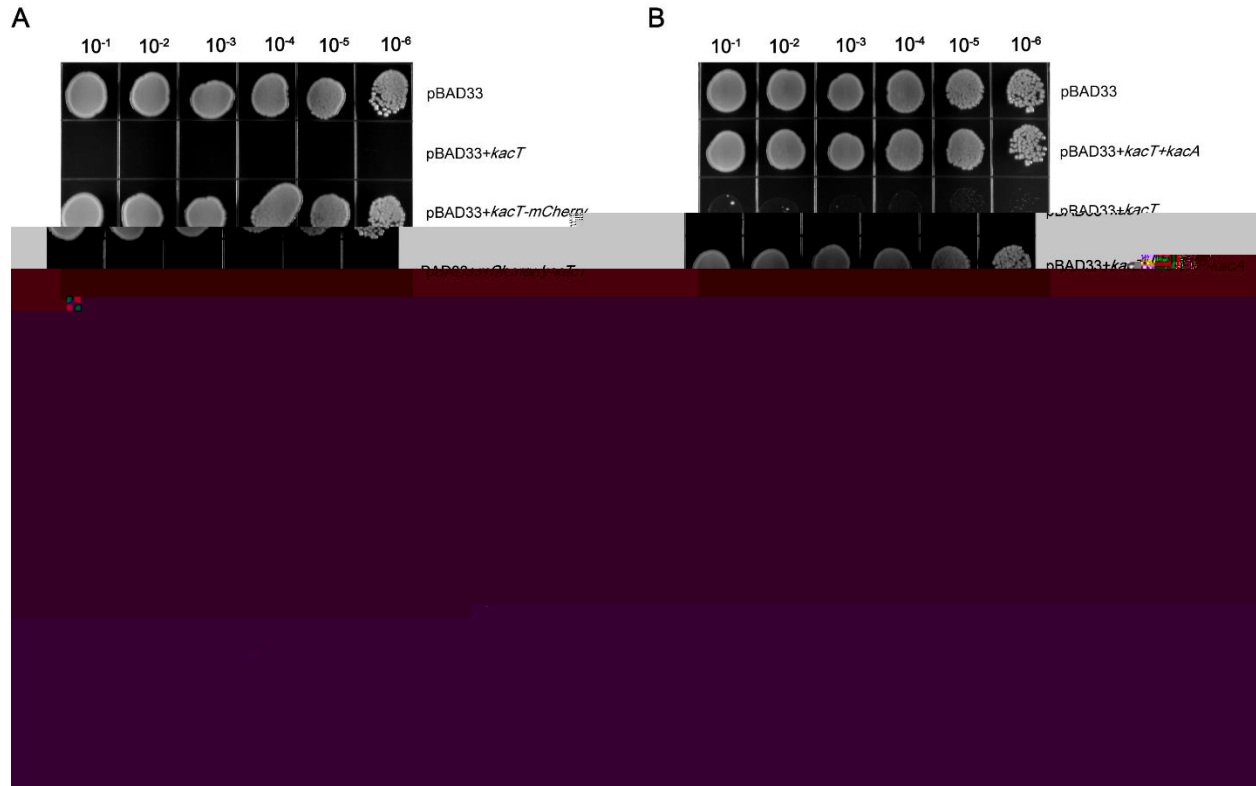
F

TV4G

TVG P PTT

T





943

944 **Figure S2.**

**A-C**

945

*!*      *T*                      *TV4G*

944

947

**D**                      *!*      *T*

976

*TV4G TVM*                      *TV4G*                      *TVM*

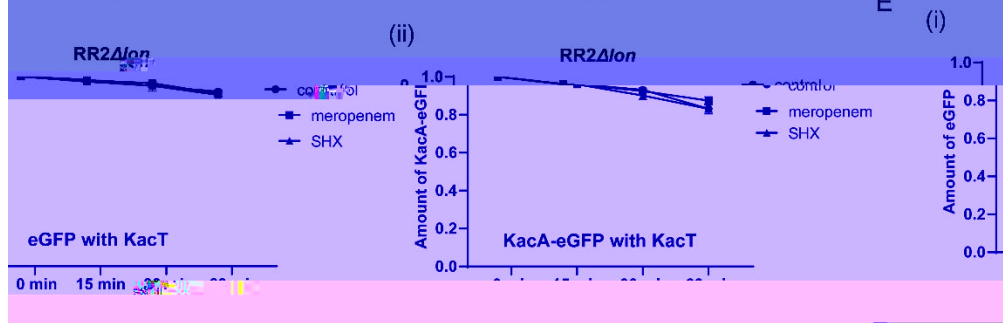
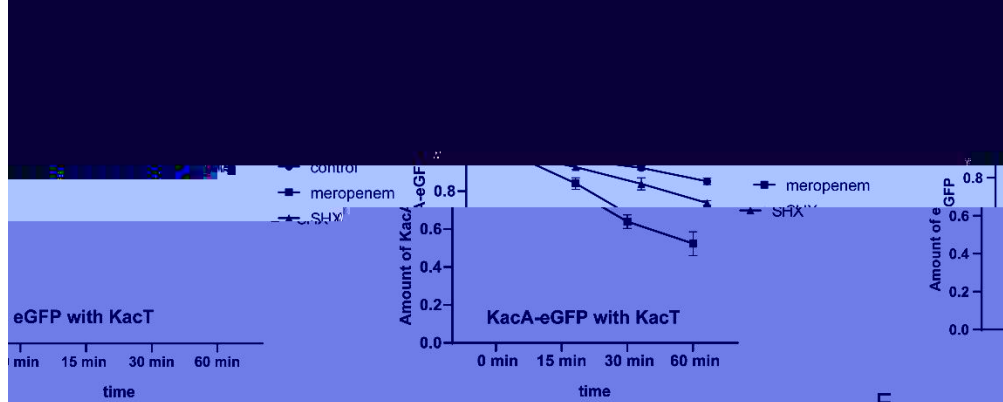
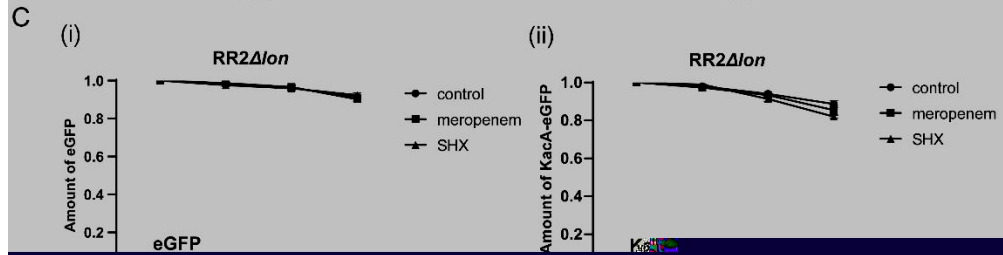
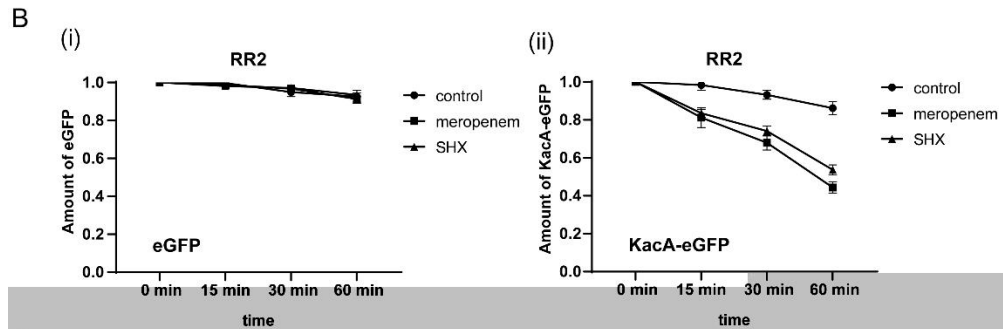
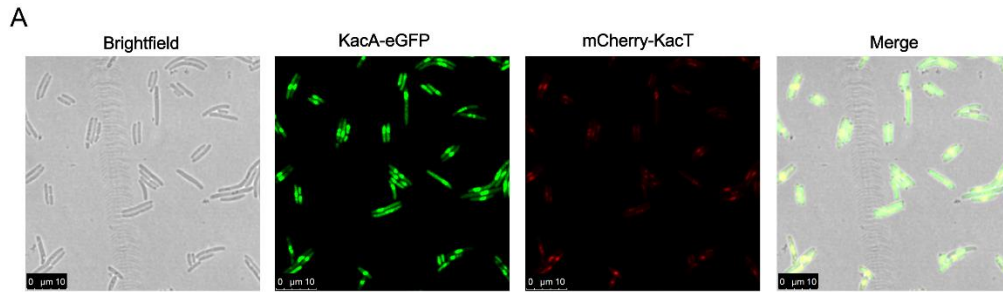
979

970

*TV4*      *TVG*

971

972



973

974 **Figure S3.**

**(A)**

975

974 *8!V*

977 *8!V*

066

069

060 **(B-C)**

061 **(D-E)** °C

062

063

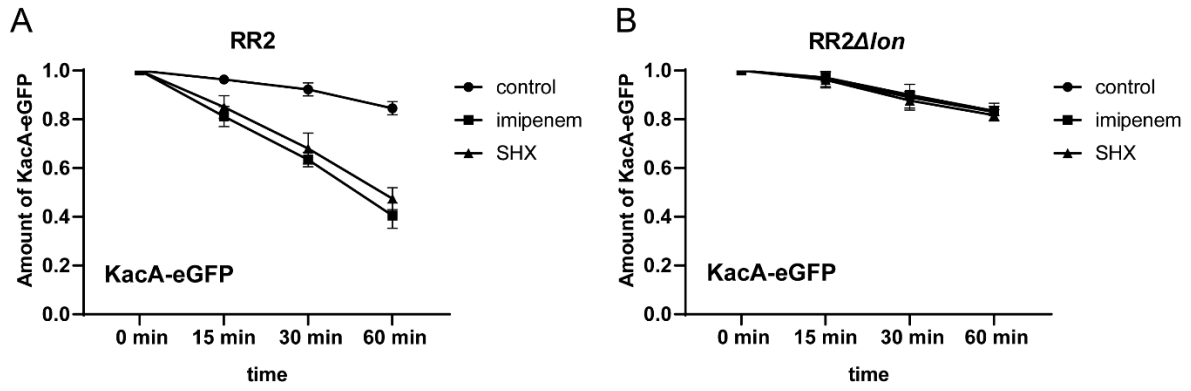
064

065

064

067

096



099

090 **Figure S4.**

091

**A**

**B**

092

!

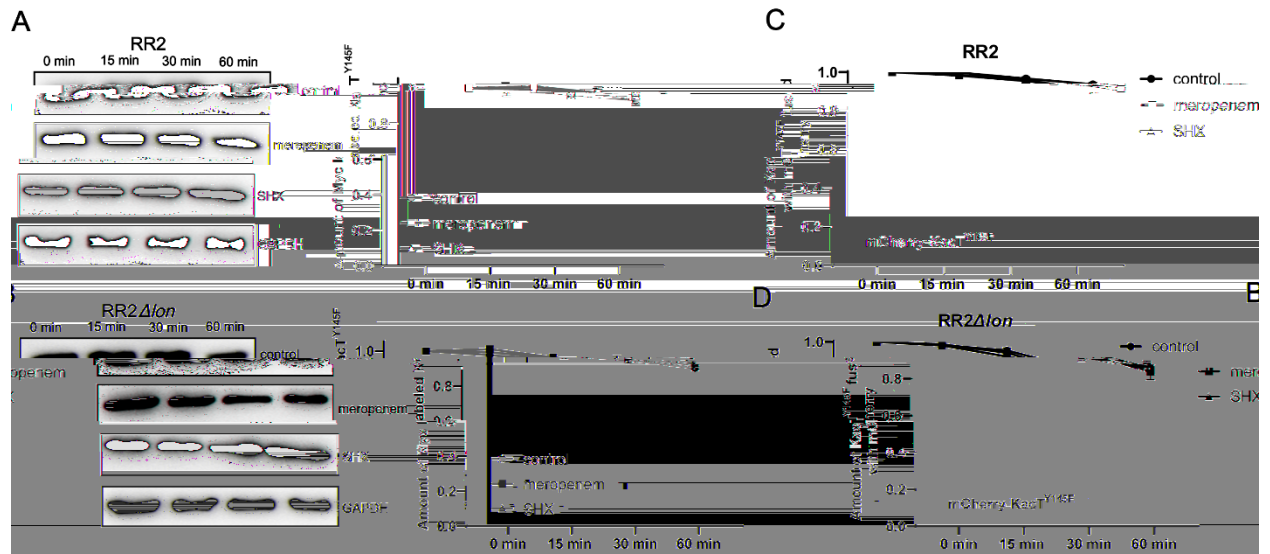
T

093

094

095

094



097

006 **Figure S5.**

009

000 (A-B)

(C-D)

001

002

003

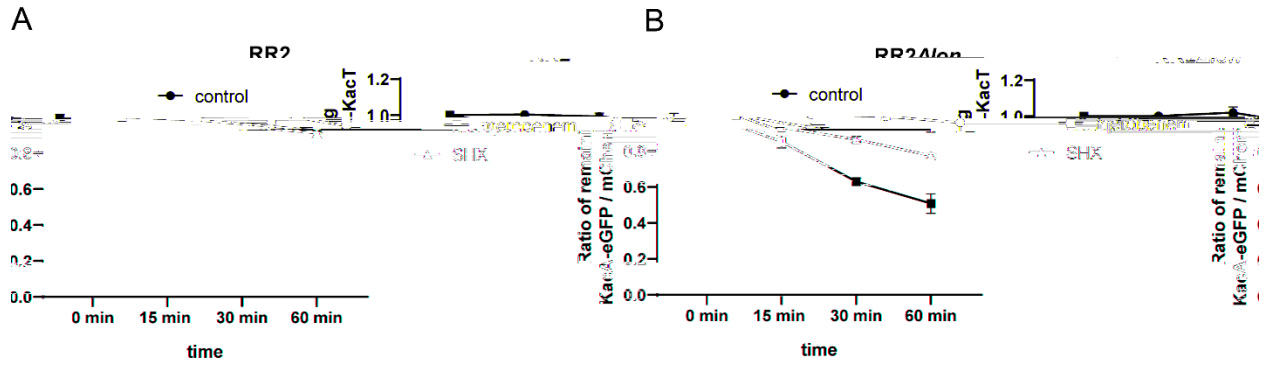
004

005

004

007

016



019

010 **Figure S6.**

011

**(A)**

**(B)**

012

013

°C

014

015

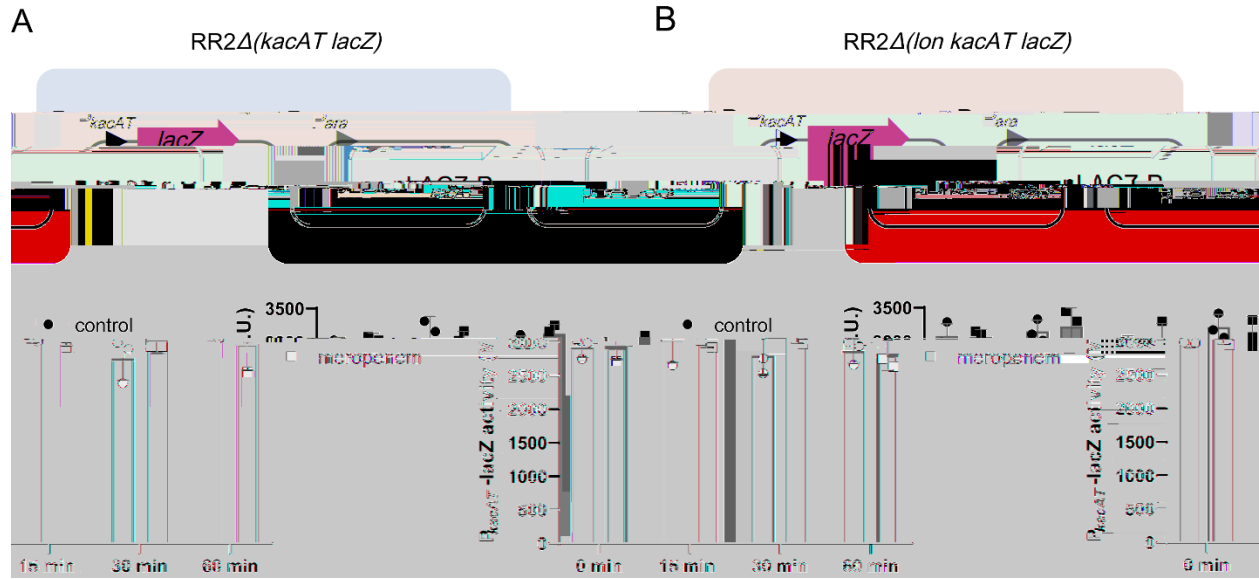
014

017

026

029

020



021

022 **Figure S7.**

TV4 G

TVM

TV4 G

023 TV4 G

TVM

TV4 G

024 TV4 G

025 TV4 G TVM (A)

TV4 G TVM (B)

024

027

036

039

030



031 **References**

032 **1**

033 4 T A V V4V E

034 **28**

035 **2** T 8 V V TV

034 A V V4V E **46**

037

046 **3**

049 4 V E **56**

040

041 **4** T

042 T T

043

044 4 V 6 **70**

045 **5** T \* \*

044 5TV **177**

047

056